AIP | Applied Physics Letters

Resonance fluorescence from a telecom-wavelength quantum dot

R. Al-Khuzheyri, A. C. Dada, J. Huwer, T. S. Santana, J. Skiba-Szymanska, M. Felle, M. B. Ward, R. M. Stevenson, I. Farrer, M. G. Tanner, R. H. Hadfield, D. A. Ritchie, A. J. Shields, and B. D. Gerardot

Citation: Applied Physics Letters **109**, 163104 (2016); doi: 10.1063/1.4965845
View online: http://dx.doi.org/10.1063/1.4965845
View Table of Contents: http://scitation.aip.org/content/aip/journal/apl/109/16?ver=pdfcov
Published by the AIP Publishing

Resonance fluorescence from a telecom-wavelength quantum dot

R. Al-Khuzheyri,[1,a)] A. C. Dada,[1,a)] J. Huwer,[2,a)] T. S. Santana,[1] J. Skiba-Szymanska,[2] M. Felle,[2,3] M. B. Ward,[2] R. M. Stevenson,[2] I. Farrer,[4,b)] M. G. Tanner,[1] R. H. Hadfield,[5] D. A. Ritchie,[4] A. J. Shields,[2] and B. D. Gerardot[1]

[1]*Institute for Photonics and Quantum Sciences, SUPA, Heriot-Watt University, Edinburgh EH14 4AS, United Kingdom*

[2]*Toshiba Research Europe Limited, Cambridge Research Laboratory, 208 Cambridge Science Park, Milton Road, Cambridge CB4 0GZ, United Kingdom*

[3]*Centre for Advanced Photonics and Electronics, University of Cambridge, J. J. Thomson Avenue, Cambridge CB3 0FA, United Kingdom*

[4]*Cavendish Laboratory, University of Cambridge, J. J. Thomson Avenue, Cambridge CB3 0HE, United Kingdom*

[5]*School of Engineering, University of Glasgow, Rankine Building, Oakfield Avenue, Glasgow G12 8LT, United Kingdom*

(Received 7 July 2016; accepted 8 October 2016; published online 20 October 2016)

We report on resonance fluorescence from a single quantum dot emitting at telecom wavelengths. We perform high-resolution spectroscopy and observe the Mollow triplet in the Rabi regime—a hallmark of resonance fluorescence. The measured resonance-fluorescence spectra allow us to rule out pure dephasing as a significant decoherence mechanism in these quantum dots. Combined with numerical simulations, the experimental results provide robust characterisation of charge noise in the environment of the quantum dot. Resonant control of the quantum dot opens up new possibilities for the on-demand generation of indistinguishable single photons at telecom wavelengths as well as quantum optics experiments and direct manipulation of solid-state qubits in telecom-wavelength quantum dots. *Published by AIP Publishing.* [http://dx.doi.org/10.1063/1.4965845]

Resonance fluorescence (RF) is a result of coherent interaction between an electromagnetic field and a two-level atomic system.[1,2] The ability to access the emission resulting from resonant excitation of a quantum dot (QD)[3] has been shown to furnish unique possibilities to investigate intriguing quantum optical effects in solid-state systems, such as non-classical light generation manifesting near-ideal antibunching,[4–6] entanglement,[7] squeezing,[8] and quantum interference and Rabi-oscillations.[9,10] These can, in turn, be harnessed for quantum information science. Quantum communication networks having nodes consisting of stationary matter qubits interconnected by flying photonic qubits[11] will require telecom photons to enable long-distance applications. This makes a coherent interface of quantum dot spins with telecom wavelength photons particularly desirable. Also, due to considerably reduced decoherence effects under resonant excitation, the best single-photon sources in terms of demonstrated indistinguishability, purity, on-demand operation and brightness are based on QD RF.[4–6,10] While QD single-photon emission occurs under incoherent pumping provided by nonresonant excitation, the latter also typically generates extra carriers in the host material. This leads to inhomogeneous broadening of the emission from spectral wandering due to charge fluctuations,[12–14] as well as time jitter between photon absorption and emission due to an uncontrolled step of non-radiative relaxation to the exciton state before recombination,[15] making RF preferable for applications exploiting single photons.

Despite the promise that telecom-QD RF offers, the previous work on QD RF has been limited to QDs emitting at $<1\,\mu$m, where losses in silica fiber are high such that long-distance quantum communication protocols[16] become unfeasible. In particular, QDs emitting at $\lambda \sim 950$ nm have been demonstrated extensively as bright sources of coherently-generated indistinguishable single photons[4–6,10,17–21] and as a bright source of entangled photon-pairs[7] via resonant excitation. Translating this progress to QDs emitting in the telecommunication O-band ($\lambda \sim 1310$ nm) or C-band ($\lambda \sim 1550$ nm) has proved challenging. Also, while QD spin-photon entanglement has been demonstrated,[22,23] including the extra complexity of downconversion to telecom wavelengths,[24] actual observation of fluorescence due to resonant interaction between a telecom-wavelength photon and a quantum dot is yet to be reported. Even so, the studies of telecom QDs under non-resonant excitation have characterised their confinement and spin properties[25] and demonstrated their potential as sources of single indistinguishable[26,27] and entangled photons.[28] Here, we demonstrate RF from a single QD emitting in the telecom O-band. In spite of the considerable charge noise in the environment of the QD, we observe nearly transform-limited linewidths for the central incoherent peak of the Mollow triplet. This signifies negligible pure dephasing in the QD.

The device was grown on a GaAs substrate by molecular beam epitaxy. The InAs-QD layer lies in a quantum well located within the intrinsic region of a *p-i-n* diode. The device contains a weak planar cavity consisting of AlGaAs/GaAs distributed Bragg reflectors for improved collection efficiency. The QDs are located in 3-μm-diameter apertures in a 100-nm-thick evaporated Al layer covering the surface of the device to facilitate navigation to the individual QDs. A

[a)]R. Al-Khuzheyri, A. C. Dada, and J. Huwer contributed equally to this work.

[b)]Present address: Department of Electronic and Electrical Engineering, University of Sheffield, Sheffield S1 3JD, United Kingdom.

similar QD has been described in a previous study based on nonresonant excitation.[28] Measurements were performed at 4 K using a high-numerical-aperture confocal-microscope setup for single-QD spectroscopy. The scattered laser light was suppressed by using orthogonal linear polarizers in the excitation and collection arms of a confocal microscope with typical extinction ratios $>10^6$. A tunable continuous-wave (CW) laser diode was used for resonant excitation. For photon counting, we used both NbTiN superconducting-nanowire single-photon detectors (SNSPD)[29] and a cooled InGaAs single-photon avalanche diode (SPAD) having a peak efficiency of ~20% at ~1310 nm for benchmarking.

First, we acquire a micro-photoluminescence (μ-PL) map with a 70-μeV-resolution grating spectrometer by varying the *p-i-n* diode bias voltage under non-resonant excitation with a diode laser at $\lambda \sim 1060$ nm. In Fig. 1(a), the map clearly shows the QD neutral (X^0) and charged (X^-) exciton lines with the linewidths of ~85 μeV. This characterisation allows the tuning of the resonant-excitation laser to the desired QD transition for the RF measurements. Furthermore, we obtain the lifetime for X^0 from time-resolved μ-PL measurements to be $T_1 = 1.394(6)$ ns. As measured using a Mach-Zehnder interferometer, the total coherence time under non-resonant excitation is $T_{2,\mathrm{nres}} = 89(8)$ ps. We base RF investigations on X^0.

By obtaining detuning spectra at various excitation wavelengths, we map the RF signal over the X^0 plateau at a fixed power above saturation. The integration time for each point in the RF measurements is 5 s. Fig. 1(b) shows the peak energies as a function of *p-i-n* voltage, while Fig. 1(c) shows the integrated counts obtained from the fits to the RF detuning-spectra data acquired for a series of excitation wavelengths. The linewidth over the extent of the X^0 plateau [shown in Fig. 1(d)] tends to decrease at more positive voltages/shorter wavelengths. The X^0 plateau mapping via RF manifests a clear Stark shift. The dependence of peak energies on the electric field F (via the *p-i-n* diode bias voltage V_g) is $E_{PL} = E_0 - pF + \beta F^2$. The field, which is a function of V_0 and the thickness of the intrinsic region (d), is $F = -(V_g - V_0)/d$. In this case, $V_0 = 2.2$ V and $d = 203$ nm.[28] The permanent dipole moment (p) and the polarizability (β) are extracted from the fit as $p/e = 0.420(4)$ nm and $\beta = -0.2140(1)\ \mu\mathrm{eV/(kV/cm)}^2$. For comparison, the nonresonant-excitation (1060-nm) case gives $p/e = 0.385(1)$ nm and $\beta = -0.2290(4)\ \mu\mathrm{eV/(kV/cm)}^2$. We believe these small differences are due to additional charging of the host semiconductor matrix induced by nonresonant optical excitation.

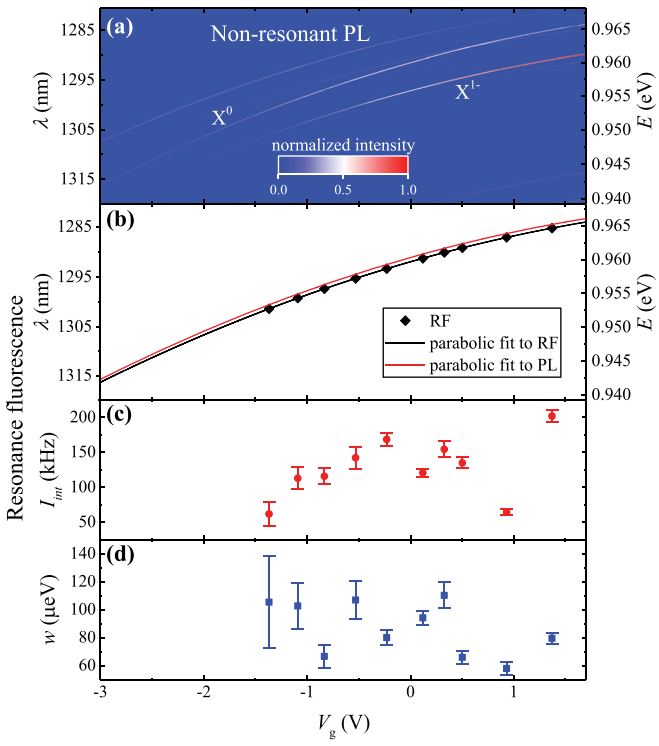

FIG. 1. (a) Microphotoluminescence-voltage map. Spectra collected as a function of the applied diode bias from a single QD within the intrinsic region of a *p-i-n* diode under 1060-nm excitation. The two lines of interest correspond to X^0 and X^- emissions from a single QD. Exciton plateau mapping in resonance fluorescence. (b) Resonance energies showing Stark shifts with permanent dipole moment $p/e = 0.420(4)$ nm and polarizability $\beta = -0.2140(1)\ \mu\mathrm{eV/(kV/cm)}^2$ for RF. PL is plotted for comparison. (c) Integrated RF counts (I_{int}) and (d) FWHM of Lorentzian fits to voltage-detuning RF spectra at different excitation wavelengths at a power of 77 nW ($\Omega = 409$ MHz).

The data points in Figs. 2(a) and 2(b) show the background-subtracted RF counts as we tune the X^0 transition through resonance with the laser using the *p-i-n* diode bias voltage. We show two examples with the resonant excitation laser and voltage across the diode set to $\lambda = 1285.28200$ nm and $V_g = 1.371$ V, respectively [due to reduced linewidths in detuning spectra, see Figs. 1(a) and 1(d)], at powers, respectively, below and above saturation. Fig. 2(c) shows that the detuning-spectra linewidth w is essentially independent of the excitation power. This is expected since the resonant laser does not charge the defects surrounding the QD. At very high excitation powers, we observe the onset of power broadening superseding charge noise. We quantify the charge noise by a characteristic width parameter w_n, which is approximately equal to the width of the detuning spectra w [see Fig. 2(c)], since $w_n \gg 1/T_1$. We demonstrate that the RF counts manifest saturation behaviour in Figs. 2(d) and 2(e), which show the (background-subtracted) RF counts plotted with the background counts and the corresponding signal-to-background ratios (SBR). Due to large w_n, the two-level system does not fully saturate at the accessible excitation powers [red curve in Fig. 2(d)]. We observe SBRs of $\lesssim 3$ [Fig. 2(e)] and suspect that background counts are mainly due to scattering of the excitation laser light off the structured sample surface. We note briefly that the characteristic double peak for X^0 corresponding to its fine-structure splitting [FSS = 109(4) μeV at $V_g = 1.371V$ in non-resonant PL] is not observable in these RF detuning spectra, possibly as a result of the diminished visibility of a smaller-intensity line due to non-orthogonal fine-structure states.[30]

We perform high-resolution spectroscopy of the RF from the QD using a Fabry-Pérot interferometer (FPI) with a 5-GHz free-spectral range and 33-MHz resolution. The integration time for each FPI measurement is ~20 min. The inelastically scattered component of the acquired FPI spectra, as shown in Fig. 3(a), clearly reveals the Mollow triplet[31] with a linear dependence of Rabi splitting on the square root of excitation power [Fig. 3(b)]–a quintessential feature of RF from a two-level system. We subtracted the narrow-linewidth elastic peak[32–34] that was contaminated by a background laser signal.

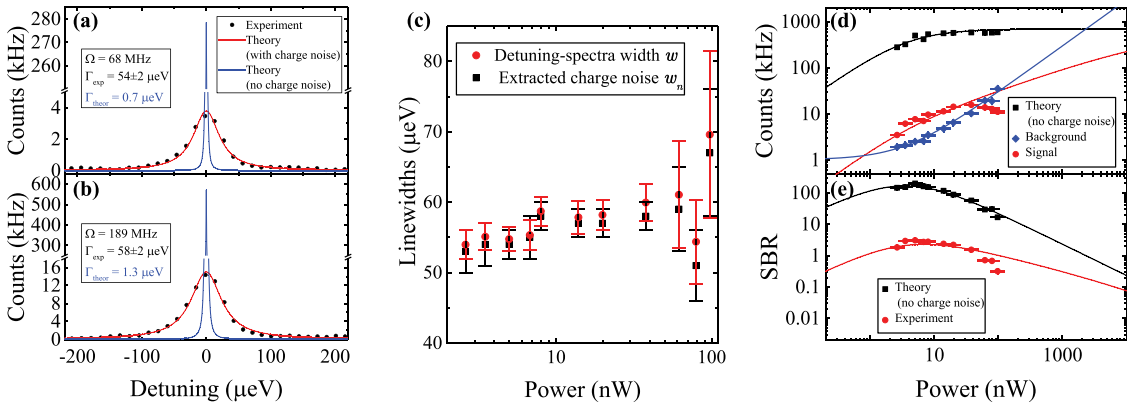

FIG. 2. (a) and (b) Resonance fluorescence detuning spectra collected from the QD X^0 state with the laser background subtracted. Detuning spectra obtained analytically using the master equation method with the charge noise parameter free was fitted to the data (red) and the case with no charge noise (blue) plotted for comparison. The scans were performed for diode bias voltages 1.3–1.45 V in 5-mV steps. (c) Linewidths of detuning spectra and extracted charge noise. Red dots: overall linewidth observed in detuning spectra; black squares: corresponding charge noise characteristic width. (d) and (e) Power dependence of resonance fluorescence counts. The amplitude of the Lorentzian fits to the background-subtracted RF voltage detuning spectra at $\lambda = 1285.28200$ nm is plotted as a function of excitation power. Represented are background-subtracted signal (red dots), background counts measured off resonance (blue dots), charge-noise-corrected experimental data (black squares) and theoretical saturation curves for the corresponding cases (solid lines). (e) shows SBR power dependence.

Finally, we demonstrate the use of RF to probe the effect of charge noise[12–14] in the telecom-wavelength QD sample. We model this by calculating the RF spectra for a 2-level system using the master-equation method,[1,2] including the effects of dephasing due to spontaneous emission, pure dephasing, and slow charge noise. This enables us to obtain an analytical result for the detuning spectra with which we fit the data [e.g., red curves in Figs. 2(a)–2(c)]. By simulating the high-resolution (FPI) RF spectra, we obtain numerical results corresponding to various amounts of charge noise w_n, as shown in Fig. 3(c), showing how charge noise broadens the side peaks of the Mollow triplet in relation to $1/T_1$. In modelling charge noise, we assume $T_1 \ll T_n \ll T_{\text{exp}}$,[13,14,33] where T_{exp} is the experiment acquisition time, and $T_n \sim 1$ ms is the timescale of spectral fluctuations due to charge noise. The combination of our experimental RF data and numerical results show that charge noise at timescales much longer than T_1 manifests in the voltage-detuning spectra as a characteristic broadening of the total linewidth [Figs. 2(a)–2(c)]. In the high-resolution FPI spectra, the charge noise primarily broadens the sidebands of the Mollow triplet [Fig. 3(c)]. Crucially, we find that the width of the central peak in our Mollow-triplet data [$\Gamma_{c,\text{min}} = 0.124(5)$ GHz] is consistent with the case of negligible pure dephasing ($T_{2,\text{res}} \approx 2T_1 \approx 2.6\text{ns} \gg T_{2,\text{nres}} \approx 90$ ps).

In summary, we present an experimental demonstration of RF from a single QD emitting at telecom wavelengths ($\lambda \approx 1300$ nm). We observe the Mollow triplet emission–a key signature of RF–with Rabi splitting showing the expected square-root dependence on excitation power, and demonstrate a contrast in dephasing times between the resonant and non-resonant excitations. Crucially, the near transform-limited linewidths observed in the central peak of the Mollow-triplet RF spectra confirm negligible pure dephasing in these QDs. We also characterise the charge noise in our sample using RF. In future work we expect that charge noise can be minimised through improved sample design and fabrication. The results pave the way for directly interfacing stationary matter qubits with telecom wavelength photons, highly-coherent single-photon emission, on-demand generation of indistinguishable photons and polarization-entangled photon pairs via RF at telecom wavelengths.

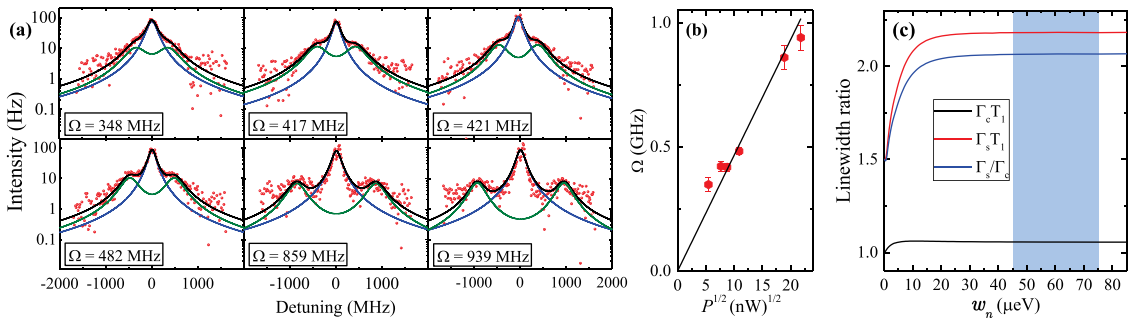

FIG. 3. (a) Observation of Mollow triplet in high-resolution telecom resonance-fluorescence spectra. The inelastically scattered component of the spectra is shown for six different excitation powers corresponding to the indicated Rabi frequencies Ω. The plots show the QD X^0 RF filtered through the FPI as a function of the FPI detuning (red dots). Lorentzian fit components: the side peaks (green curve), the central peak (blue curve), and the total (black curve). (b) The Rabi splitting/frequency as a function of the square root of excitation power showing the expected linear dependence. (c) Theoretical simulation of FPI-spectra line-widths (FWHM) of the central (Γ_c) and either of the side peaks (Γ_s) as a function of w_n obtained from numerical simulation of the master equation. $w_n = 0$ corresponds to the ideal case without charge noise. We show the respective ratios for linewidths and comparison with the transform limited case $\Gamma_c T_1 = 1$. We are unable to extract precise values for charge noise contributions from the FPI data in (a) because the measurements lie in the shaded region in (c).

This work was funded by the EPSRC (Grant Nos. EP/I023186/1, EP/K015338/1, EP/M013472/1, EP/G03673X/1, EP/K0153338/1, EP/I036273/1, and EP/J007544/1) and an ERC Starting Grant (No. 307392). B.D.G. and R.H.H. acknowledge the Royal Society University Research Fellowships. R.H.H. thanks Professor V. Zwiller and Dr. S. Dorenbos for providing the SNSPD detector chip.

[1]R. Loudon, *The Quantum Theory of Light* (OUP, Oxford, 2000).
[2]M. O. Scully and M. S. Zubairy, *Quantum Optics* (Cambridge University Press, 1997).
[3]A. Muller, E. B. Flagg, P. Bianucci, X. Y. Wang, D. G. Deppe, W. Ma, J. Zhang, G. J. Salamo, M. Xiao, and C. K. Shih, Phys. Rev. Lett. **99**, 187402 (2007).
[4]X. Ding, Y. He, Z. C. Duan, N. Gregersen, M. C. Chen, S. Unsleber, S. Maier, C. Schneider, M. Kamp, S. Höfling, C.-Y. Lu, and J.-W. Pan, Phys. Rev. Lett. **116**, 020401 (2016).
[5]J. C. Loredo, N. A. Zakaria, N. Somaschi, C. Anton, L. de Santis, V. Giesz, T. Grange, M. A. Broome, O. Gazzano, G. Coppola, I. Sagnes, A. Lemaitre, A. Auffèves, P. Senellart, M. P. Almeida, and A. G. White, Optica **3**, 433 (2016).
[6]N. Somaschi, V. Giesz, L. De Santis, J. C. Loredo, M. P. Almeida, G. Hornecker, S. L. Portalupi, T. Grange, C. Anton, J. Demory, C. Gomez, I. Sagnes, N. D. Lanzillotti-Kimura, A. Lemaître, A. Auffèves, A. G. White, L. Lanco, and P. Senellart, Nat. Photonics **10**, 340 (2016).
[7]M. Müller, S. Bounouar, K. D. Jöns, M. Glässl, and P. Michler, Nat. Photonics **8**, 224 (2014).
[8]C. Schulte, J. Hansom, A. E. Jones, C. Matthiesen, C. Le Gall, and M. Atature, Nature **525**, 222 (2015).
[9]J. R. Schaibley, A. P. Burgers, G. A. McCracken, D. G. Steel, A. S. Bracker, D. Gammon, and L. J. Sham, Phys. Rev. B **87**, 115311 (2013).
[10]A. C. Dada, T. S. Santana, R. N. Malein, A. Koutroumanis, Y. Ma, J. M. Zajac, J. Y. Lim, J. D. Song, and B. D. Gerardot, Optica **3**, 493 (2016).
[11]A. Delteil, Z. Sun, W.-B. Gao, E. Togan, S. Faelt, and A. Imamoğlu, Nat. Phys. **12**, 218 (2016).
[12]J. Houel, A. V. Kuhlmann, L. Greuter, F. Xue, M. Poggio, B. D. Gerardot, P. A. Dalgarno, A. Badolato, P. M. Petroff, A. Ludwig, D. Reuter, A. D. Wieck, and R. J. Warburton, Phys. Rev. Lett. **108**, 107401 (2012).
[13]A. V. Kuhlmann, J. Houel, A. Ludwig, L. Greuter, D. Reuter, A. D. Wieck, M. Poggio, and R. J. Warburton, Nat. Phys. **9**, 570 (2013).
[14]C. Matthiesen, M. J. Stanley, M. Hugues, E. Clarke, and M. Atatüre, Sci. Rep. **4**, 4911 (2014).
[15]C. Santori, D. Fattal, J. Vučković, G. S. Solomon, and Y. Yamamoto, New J. Phys. **6**, 89 (2004).
[16]H. J. Kimble, Nature **453**, 1023 (2008).
[17]T. Huber, A. Predojević, D. Föger, G. Solomon, and G. Weihs, New J. Phys. **17**, 123025 (2015).
[18]C. Matthiesen, M. Geller, C. H. H. Schulte, C. L. Gall, J. Hansom, Z. Li, M. Hugues, E. Clarke, and M. Atatüre, Nat. Commun. **4**, 1600 (2013).
[19]S. Ates, S. M. Ulrich, S. Reitzenstein, A. Löffler, A. Forchel, and P. Michler, Phys. Rev. Lett. **103**, 167402 (2009).
[20]L. Monniello, A. Reigue, R. Hostein, A. Lemaitre, A. Martinez, R. Grousson, and V. Voliotis, Phys. Rev. B **90**, 041303 (2014).
[21]A. Bennett, J. Lee, D. Ellis, T. Meany, E. Murray, F. Floether, J. Griffths, I. Farrer, D. Ritchie, and A. Shields, Science Advances **2**, e1501256 (2016).
[22]J. R. Schaibley, A. P. Burgers, G. A. McCracken, L. M. Duan, P. R. Berman, D. G. Steel, A. S. Bracker, D. Gammon, and L. J. Sham, Phys. Rev. Lett. **110**, 167401 (2013).
[23]W. Gao, P. Fallahi, E. Togan, A. Delteil, Y. Chin, J. Miguel-Sanchez, and A. Imamoğlu, Nat. Commun. **4**, 2744 (2013).
[24]K. De Greve, L. Yu, P. L. McMahon, J. S. Pelc, C. M. Natarajan, N. Y. Kim, E. Abe, S. Maier, C. Schneider, M. Kamp, S. Höfling, R. H. Hadfield, A. Forchel, M. M. Fejer, and Y. Yamamoto, Nature **491**, 421 (2012).
[25]L. Sapienza, R. Al-Khuzheyri, A. C. Dada, A. Griffiths, E. Clarke, and B. D. Gerardot, Phys. Rev. B **93**, 155301 (2016).
[26]J.-H. Kim, T. Cai, C. J. Richardson, R. P. Leavitt, and E. Waks, Optica **3**, 577 (2016).
[27]M. Felle, J. Huwer, R. M. Stevenson, J. Skiba-Szymanska, M. B. Ward, I. Farrer, R. V. Penty, D. A. Ritchie, and A. J. Shields, Appl. Phys. Lett. **107**, 131106 (2015).
[28]M. Ward, M. Dean, R. Stevenson, A. Bennett, D. Ellis, K. Cooper, I. Farrer, C. Nicoll, D. Ritchie, and A. Shields, Nat. Commun. **5**, 3316 (2014).
[29]M. G. Tanner, C. M. Natarajan, V. K. Pottapenjara, J. A. O'Connor, R. J. Warburton, R. H. Hadfield, B. Baek, S. Nam, S. N. Dorenbos, E. B. Ureña, T. Zijlstra, T. M. Klapwijk, and V. Zwiller, Appl. Phys. Lett. **96**, 221109 (2010).
[30]Y.-J. Wei, Y. He, Y.-M. He, C.-Y. Lu, J.-W. Pan, C. Schneider, M. Kamp, S. Höfling, D. P. S. McCutcheon, and A. Nazir, Phys. Rev. Lett. **113**, 097401 (2014).
[31]B. R. Mollow, Phys. Rev. **188**, 1969 (1969).
[32]C. Matthiesen, A. N. Vamivakas, and M. Atature, Phys. Rev. Lett. **108**, 093602 (2012).
[33]K. Konthasinghe, J. Walker, M. Peiris, C. K. Shih, Y. Yu, M. F. Li, J. F. He, L. J. Wang, H. Q. Ni, Z. C. Niu, and A. Muller, Phys. Rev. B **85**, 235315 (2012).
[34]H. S. Nguyen, G. Sallen, C. Voisin, P. Roussignol, C. Diederichs, and G. Cassabois, Appl. Phys. Lett. **99**, 261904 (2011).